

Luminescence of PbCl₂ and PbBr₂ Single Crystals

II. Luminescence and EPR of uv Irradiated Crystals

W. C. DE GRUIJTER AND J. KERSSSEN

*Solid State Department, University of Utrecht,
Sorbonnelaan 4, Utrecht, The Netherlands*

Received March 30, 1972

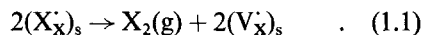
PbCl₂ and PbBr₂ single crystals show a red luminescence under uv excitation at temperatures below 200°K. Furthermore, PbCl₂ shows a yellow emission at temperatures below 40°K. The centers responsible for these emissions have been investigated by EPR measurements. These measurements indicate that due to uv irradiation Pb'_{Pb}, (Pb'_{Pb})₂ and lead colloids are created. In PbCl₂, a hole center, possibly Cl'_{Cl}, is created at temperatures below 50°K. Both the concentration of the Pb'_{Pb} and the (Pb'_{Pb})₂ centers in PbCl₂ depends on the irradiation intensity; the concentration of the pair-centers increases with time after the irradiation is stopped. A similar dependence has been observed on PbBr₂ crystals cleaved and mounted in the dark, but in this case the influence of the irradiation appears to be smaller. The defects responsible for the red and yellow luminescence could be identified on the basis of temperature dependence measurements. The red luminescence of both halides is ascribed to excitation and decay of Pb'_{Pb} or (Pb'_{Pb})₂ centers, and the yellow luminescence of PbCl₂ is associated with Cl'_{Cl} centers.

1. Introduction

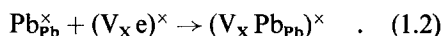
Single crystals of PbCl₂ and PbBr₂ show photoluminescence under uv excitation at low temperatures (1). The red luminescence was observed at temperatures lower than 200°K. At the same temperatures the uv irradiation of the crystals causes also a photochemical change, which is not observed in optical absorption measurements. If the crystals are warmed up, an absorption band develops, which is ascribed to colloidal lead particles (2). In view of these phenomena we tentatively associated the red luminescence of PbCl₂ and PbBr₂ single crystals with centers created by uv irradiation. The present paper reports on the centers which cause the red luminescence of PbCl₂ and PbBr₂ and the yellow luminescence of PbCl₂. The following investigations were carried out:

- a. measurements of the luminescence excitation and -emission spectra,
- b. EPR measurements of luminescence centers,
- c. measurements of the temperature dependence of the luminescence and the EPR signals.

It is well known that PbCl₂ and PbBr₂ decompose under uv irradiation at room temperature (3-7). Verwey (2, 8) investigated the photochemical decomposition on single crystals in this laboratory. This author proposed the following mechanism for the photolysis at room temperature, also on the basis of EPR measurements (10): an absorbed photon creates an electron hole pair. The hole h⁺ diffuses to the surface and is trapped at a surface halide ion (X_X[•])_s.¹ Two halogen atoms give a halogen molecule which desorbs from the surface



The anion vacancies formed at the surface diffuse into the crystal. Anion vacancies may also be created by a Pooley-Hersh mechanism (9, 12). Electrons are trapped at anion vacancies giving an F center structure (V_Xe)[•]. This center is not stable. It probably produces a Pb⁺ ion according to



¹ Here and throughout this paper the defect notation of Kröger is used (11). [•] = effective charge zero; ['] = effective charge +q; ['] = effective charge -q.

Aggregation of $(V_X Pb_{Pb})^{\times}$ or Pb^+ gives lead particles $(Pb)_n$ and lead ions Pb_{Pb}^{\times} . Also annihilation of V_X occurs in order to supply room for the lead particles since the lead atom has a larger radius than the lead ion (10).

2. Experimental

The single crystals used in this investigation are prepared by means of the Bridgman technique. Because of the hygroscopic character of $PbCl_2$ and $PbBr_2$, the crystals are prepared with special care to avoid adsorption and inclusion of water (17). Details of the preparation have been published elsewhere (13). Analyses by emission spectroscopy show that the impurity content is very low (17). For our investigations, platelets of 2–4 mm thickness are cleaved parallel to the (001) plane from large single crystals.

The luminescence measurements are performed with a setup described in a previous paper (17).

The EPR measurements are carried out with an X-band spectrometer (frequency 8–11 GHz) built in this laboratory. Its maximum sensitivity is about 5×10^{12} spins/gauss. The circular TE-011 EPR cavity is part of a cryostat and is provided with suprasil windows to allow uv irradiation of the sample. The sample is mounted in the center of the evacuated cavity and can be rotated around an axis perpendicular to the static magnetic field H . Details of the construction will be published elsewhere (14). The magnetic field modulation frequency is 100 kHz. The microwave frequency is measured with an HP5257A transfer oscillator. An AEG NMR gauss-meter is employed to measure $|H|$. Owing to the different locations of NMR probe and sample, the accuracy with which g values can be determined is limited to $1:10^4$.

The samples are irradiated with an Osram HBO-200/W2 high pressure mercury lamp. In order to avoid local heating and possible optical bleaching, filters are used. We mainly used a Schott UV-R-250 interference reflection filter and the blue glass filters UG5 (Schott and Gen.; maximum transmittance wavelength 330 nm) and 18 A (Kodak; maximum transmittance wavelength 360 nm). For the HBO lamp in combination with the UV-R-250 filter, the intensity of the radiation on the sample in the cryostat was $\sim 10^{16}$ photons $cm^{-2} s^{-1}$. In some experiments neutral density filters are used to reduce the intensity of the radiation.

3. The EPR results

3.1 General

At room temperature no EPR signals were observed in any of the samples of $PbCl_2$ and $PbBr_2$, investigated before, during or after uv irradiation. The paramagnetic centers could be created at low temperatures by irradiation within the investigated region of strong absorption of the crystals. The absorption spectra of $PbCl_2$ and $PbBr_2$ are presented in Figs. 6 and 7.

3.2 The EPR Spectra of $PbCl_2$

Unirradiated samples did not show an EPR signal at 77°K. At this temperature a weak EPR signal developed after some minutes of irradiation (intensity 10^{16} photons $cm^{-2} s^{-1}$) (36). When the irradiation was stopped, the strength of this signal increased with time. Figure 1 (spectrum A) shows this signal, which was registered about 1 hr after irradiation. Repeated irradiation with the same intensity reduced the strength of the A signal with a factor of about 30. Every time the irradiation was interrupted the signal strength increased slowly with time in the same way, whereas the strength was reduced to the 3% level if the irradiation was applied again (cf. Fig. 2). Repeated irradiation with an intensity of about 10^{14} photons $cm^{-2} s^{-1}$ gave only a slight decrease of the A signal strength. The strength of the A signal increased if the sample was cooled down to

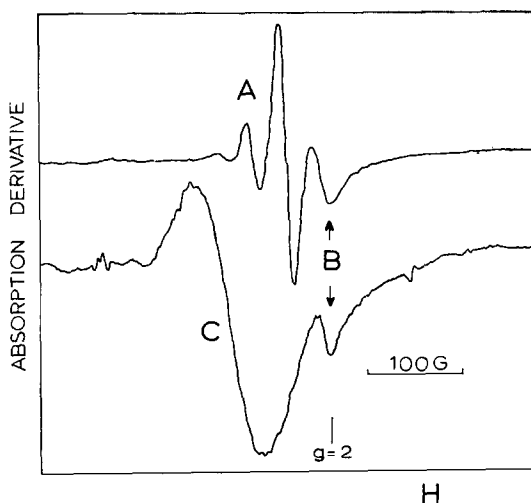


FIG. 1. Typical recorder tracings of the derivatives of the A, B, and C microwave absorption vs magnetic field strength in $PbCl_2$ at 9.4 GHz and 77°K (upper trace) and 10°K (lower trace).

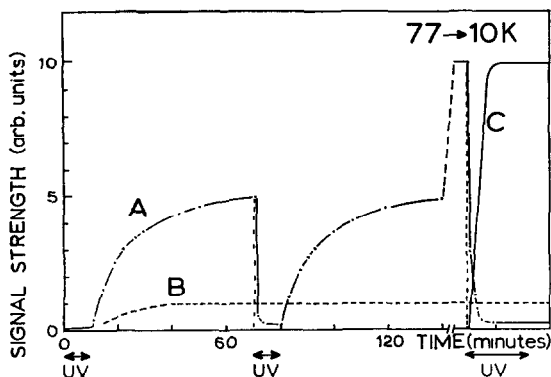


FIG. 2. Intensity of the A, B, and C EPR signals in PbCl₂ as a function of time, during and after uv irradiation at 77 and 10°K for A and B and at 10°K for C (UV = irradiation period).

10°K (cf. Figs. 2 and 3). A subsequent uv irradiation reduced its strength in an irreversible way (cf. Fig. 2). If, thereupon, the sample was warmed up to 77°K, the original increase of the A signal strength was measured again.

After warming up the sample to room temperature (bleaching) and subsequent cooling down no EPR signals are found at 77°K. In addition, irradiation produces the same results as described above. When after thermal bleaching the sample is cooled down directly to 10°K subsequent irradiation produces the B and C signals (see Fig. 1) and possibly a weak A signal. After a subsequent warmup to 77°K the A signal returned without further irradiation. The entire process was completely reproducible and was observed on practically all the PbCl₂ samples.

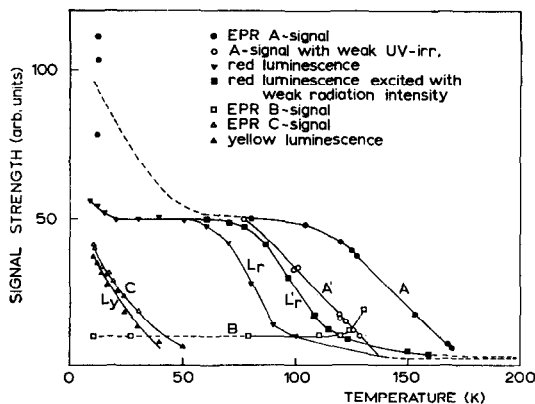


FIG. 3. Temperature dependences of the red luminescence (L_r and L'_r), the yellow luminescence (L_y), the EPR signal A without (A), and during weak (A') uv irradiation and the EPR signals B(B) and C(C) in PbCl₂.

Following the first irradiation at 77°K, as well as 10°K, usually a B signal developed (cf. Figs. 1 and 2). Its strength did not change significantly as a function of time or irradiation intensity.

Samples cooled down to 10°K showed another EPR signal due to irradiation (cf. Fig. 1, signal C) at this temperature. Its strength increased up to a certain level in some minutes of irradiation and remained practically constant after irradiation.

The temperature dependence of the A, B, and C signals, measured without irradiation, is given in Fig. 3. Only curve A' was measured during uv irradiation with weak intensity (10¹⁴ photons cm⁻² s⁻¹).

The Profile of the EPR Signals of PbCl₂

The A signal consists of five equally spaced gaussian-shaped lines. The last component is usually hidden in the B signal (cf. Fig. 1). The mutual distance of the lines is 35 G, which is independent of the microwave frequency and the angle between H and the crystal axes. The ratios of the line strengths vary slightly with time and irradiation history, but are on the average

$$0.04:0.24:1:0.22:(0.04) \quad (3.2.1)$$

(accuracy ±0.01, except for the last component). The peak to peak width of these lines is 15 G. The g value of the lines is anisotropic. The angular dependence of the g values upon rotation of H in the (001) plane is given in Fig. 4.

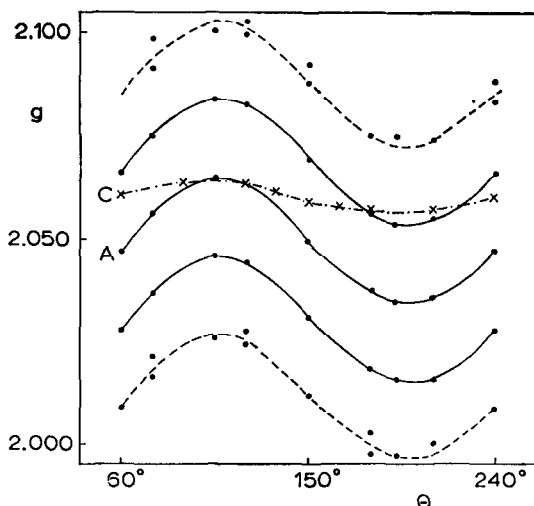


FIG. 4. The angular dependence of the g value of the EPR signals A and C in PbCl₂. Rotation around the [001] axis.

The number of centers created with a radiation intensity of $\sim 10^{16}$ photons $\text{cm}^{-2} \text{s}^{-1}$ has been calculated from a comparison with an active coal standard sample. The number of centers concerned in the A signal is, 1 hr after irradiation, about 3×10^{15} and about 10^{14} during irradiation. The penetration depth of the radiation involved is about $0.3 \mu\text{m}$ and the surface dimensions of the samples are $\sim 0.5 \text{ cm} \times 0.5 \text{ cm}$. If the centers stay in the surface layer, the aforementioned numbers of spins correspond with $\sim 4 \times 10^{20}$ centers cm^{-3} and $\sim 10^{19}$ centers cm^{-3} , respectively.

The B signal (cf. Fig. 1) is an isotropic line with a g value of 2.0024 and a peak to peak width of about 18 G. Most times this signal has a pronounced asymmetric line shape which resembles the line shapes calculated by Webb (15) for conduction electrons in spherical metal particles. In this case the concentration of centers involved is $\sim 5 \times 10^{19} \text{ cm}^{-3}$.

The C signal (cf. Fig. 1) is a rather broad (72 G) gaussian-shaped line. The g value is slightly angular dependent (cf. Fig. 4,C) when H is rotated in the (001) plane. The concentration of the centers is $\sim 10^{20} \text{ cm}^{-3}$. Several registrations of the C signal show some structure on the peaks.

3.3 The EPR Spectra of PbBr_2

Contrary to the observations at 300°K (cf. Sect. 3.1), unirradiated PbBr_2 samples cleaved and mounted in daylight showed weak EPR signals at 77°K. Their strength did not change if the samples were exposed to uv irradiation. At 77°K no EPR signals were detected, however, on unirradiated samples, cleaved and mounted in the dark.

During irradiation (intensity $\sim 10^{16}$ photons $\text{cm}^{-2} \text{s}^{-1}$) at 77°K of a PbBr_2 sample cleaved and mounted in the dark, a weak and complicated EPR spectrum developed, consisting of a large number of lines in a very broad region (about 1000 G). Among other lines an A type signal was observed (cf. Fig. 5). Repeated irradiation caused a decrease of the strength of this signal, as is the case for PbCl_2 . However, this decrease was only a factor of 2. After the irradiation was stopped, the signal strength increased in some minutes to the original level. This process could be reproduced until the entire irradiation period was about 30 min. From that time, repeated irradiation did not change the strength of the A type signal any more. This ultimate signal agrees with that measured on samples mounted in daylight. Since the low energy absorption band of PbBr_2 is

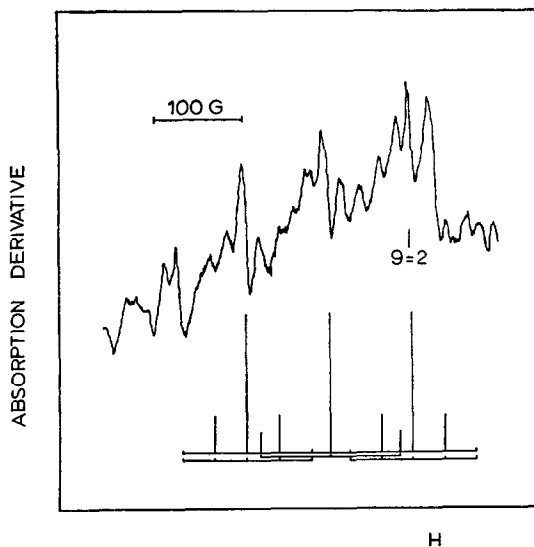


FIG. 5. The derivative of the microwave absorption as a function of the magnetic field strength for a PbBr_2 crystal at 77°K. Part of a typical recorder tracing at 9.8 GHz (upper trace). The second figure represents the analysis of the A type signal. The position of the satellites is calculated taking the same value for the hyperfine constant as found for PbCl_2 .

situated in the near uv part of the spectrum (cf. Fig. 7), it is most likely that the daylight causes the centers in these samples.

After the first irradiation the B signal shows up in most of the PbBr_2 samples. This signal exhibits the same characteristics as described for the B signal of PbCl_2 (cf. Sect. 3.2).

If the samples were cooled down to 10°K, the strength of the A and the B signal did not change significantly. Irradiation at 10°K did not destroy the centers responsible for the A type signal as is the case for PbCl_2 . Due to the small strength of the EPR signals the temperature dependence in the region 80–200°K could not be measured reproducibly with our setup.

The Profile of the EPR Signals of PbBr_2

The A type signal consists of three equidistant lines (distance 92 G) each of them surrounded by some satellites. The central line has a g value of 2.0536. The outer lines have g values of 1.9988 and 2.1081. No angular dependence could be detected. The peak to peak width of these lines is 12 G. Due to the complicated background and the small strength of the A type signal, the strength and the exact position of the satellites could not be determined uniquely. The concen-

tration of centers created in the surface layer with an irradiation intensity of 10^{16} photons $\text{cm}^{-2} \text{s}^{-1}$ is about $5 \times 10^{18} \text{ cm}^{-3}$.

The g value of the B signal is 2.0010; the concentration of centers involved is $\sim 10^{18} \text{ cm}^{-3}$.

In PbBr₂, no C type signals have been observed.

4. The Luminescence of PbCl₂ and PbBr₂

In the temperature region 10–180°K, PbCl₂ as well as PbBr₂ single crystals show three emission bands under uv excitation, viz., one in the uv part of the spectrum, a second one in the blue and a third in the red. In addition, PbCl₂ shows another two emission bands at 5°K, viz., a violet and a yellow (*I*). In preceding papers (*I*, *16*) we attributed the uv emission of both lead halides to the recombination of ³P₁ cation excitons. The temperature dependence of the blue emission of PbCl₂ and PbBr₂ is quite different (*17*). The blue emission of PbBr₂ is quenched between 10°K and 30°K, whereas that of PbCl₂ is constant up to 110°K and is quenched in the region 110–180°K.

The excitation and emission spectra of the red luminescence of PbCl₂ and PbBr₂ at 77°K are reproduced in Figs. 6 and 7. From a comparison with the absorption spectra it appears that the red emission of both halides is preferentially excited in the low energy region of the absorption spectrum, i.e., the region of the ³P₁ cation exciton absorption band (*I*). The temperature

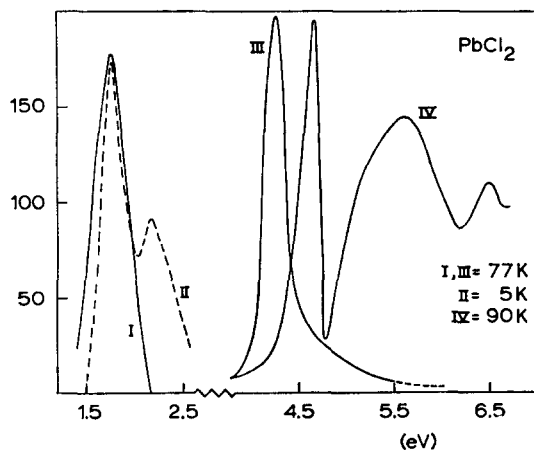


FIG. 6. Spectral energy distribution of I: The red luminescence of a PbCl₂ crystal at 77°K and II: The red and yellow luminescence at 5°K. III: Relative excitation spectrum of the red luminescence at 77°K. IV: Relative absorption spectrum of a thin layer of PbCl₂ at 90°K, taken from the measurements of Best (*28*). The curves have been plotted in arbitrary units.

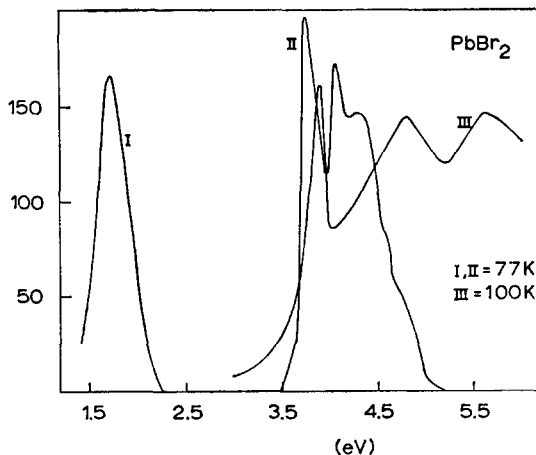


FIG. 7. I: Spectral energy distribution of the red luminescence of a PbBr₂ crystal at 77°K. II: Relative excitation spectrum of the red luminescence at 77°K. III: Relative absorption spectrum of a thin layer of PbBr₂ at 100°K taken from the measurements of Ilmas *et al.* (*29*). The curves have been plotted in arbitrary units.

dependence of the red emission of PbCl₂ is presented in Fig. 3. If the intensity of the exciting radiation was increased, the quenching temperature shifted to lower values ($I_{L_r} > I_{L_r}'$). The same holds for the temperature dependence of the EPR signal A (cf. Sect. 3.2). The red and the yellow emission band of PbCl₂ at 5°K are given in Fig. 6 and the temperature dependence of the yellow emission in Fig. 3. The excitation spectrum of the yellow luminescence nearly coincides with that of the red luminescence (*17*).

For PbBr₂, temperature dependence measurements indicated that the red luminescence is quenched in the region 100–200°K (*17*). With reference to the EPR measurements at 77°K on PbBr₂ samples cleaved and mounted in the dark, the luminescence intensity was measured on such a crystal as a function of irradiation time. The intensity decreased (about 20%) during irradiation and returned to its original level during a subsequent interruption. This experiment could be reproduced several times, whereas the signal intensity became constant after prolonged irradiation.

Optical absorption measurements at low temperatures in the transparent energy region of PbCl₂ and PbBr₂ did not show an absorption band due to the centers responsible for the red luminescence. In view of the excitation spectra involved (cf. Figs. 6 and 7) we assume that these absorption bands are situated in the energy

region of the 3P_1 cation exciton absorption bands of the compounds, respectively. The measurements of the excitation spectra of the red luminescence (see Figs. 6 and 7) in conjunction with photoconductivity measurements (23) showed that in the region of the 3P_1 cation exciton absorption band free carriers do not transport the exciting energy to the luminescence centers.

5. Discussion

5.1 The Relation between the EPR and the Luminescence Results

On the basis of the temperature dependence measurements it is improbable that the blue luminescence of $PbCl_2$ and $PbBr_2$ is associated with the EPR signal A. For $PbCl_2$, the temperature dependences of the red luminescence and of the A signal (cf. Fig. 3, L'_r and A') agree rather well. Since these plots were determined with different setups it was difficult to carry out the experiments with exactly equal radiation intensities. From these measurements we arrive at the conclusion that the red luminescence of $PbCl_2$ is associated with the center responsible for the EPR signal A. For two reasons we assume that the red luminescence of $PbBr_2$ is associated with the A type signal. First, the intensity of the red luminescence and the A type signal show corresponding variations due to irradiation (see Sect. 4). Secondly, the A type signal and the red luminescence both have disappeared above 200°K. In view of the temperature dependence measurements the yellow luminescence of $PbCl_2$ is associated with the EPR signal C (cf. Fig. 3).

5.2 The A Signal of $PbCl_2$

In this section we will show that the EPR signal A originates from exchange-coupled pairs of Pb'_{Pb} ions and from single Pb'_{Pb} ions. The electron configuration of the Pb^+ ion is $6s^2p^1$. According to Kramers' theorem the Pb'_{Pb} ground state will be a doublet. The EPR spectrum of Pb'_{Pb} is expected to consist of three equally spaced lines. The intensity ratios of the lines have been calculated with the aid of the isotope ratio. Analysis² of a typical crystal showed that the ${}^{204}Pb$, ${}^{206}Pb$, and ${}^{208}Pb$ isotopes are together

78.6% ($\pm 1\%$) abundant and the ${}^{207}Pb$ isotope 21.4%. The calculated intensity ratios are

$$0.14:1.00:0.14. \quad (5.2.1)$$

The central line of this signal originates from the ${}^{204}Pb$, ${}^{206}Pb$, and ${}^{208}Pb$ isotopes, which have no nuclear spin. The satellite on each side of the central line is due to hyperfine interaction with the ${}^{207}Pb$ isotope which has a nuclear spin $I = \frac{1}{2}$ and a nuclear moment $\mu_N = 0.5837$. The hyperfine splitting in this case is $\pm \frac{1}{2}A$ (A is the hyperfine parameter for an isolated Pb_{Pb} ion). The experimental results, however, showed that the A signal consists of five lines [see Eq. (3.2.1)]. In addition, the experimental intensity ratios of the inner three lines are not in agreement with the calculated ratios (cf. Sect. 3.2). The EPR spectrum originating from isotropic coupled Pb'_{Pb} pairs with an effective spin of 1, consists of five equally spaced lines. Now, the hyperfine splitting will be $\frac{1}{2}A(m_i + m_j)$ (18), where m_i and m_j are the nuclear magnetic quantum numbers for the two Pb'_{Pb} ions of the pair. Since the sum ($m_i + m_j$) can take the values ± 1 , $\pm \frac{1}{2}$, and 0, the hyperfine splitting amounts to $\pm \frac{1}{2}A$ and $\pm \frac{1}{4}A$. The intensity ratios of the lines making allowance for the isotope ratio are

$$0.02:0.27:1.00:0.27:0.02 \quad (5.2.2)$$

From a comparison with the experimental ratios [see Eq. (3.2.1)] it appears that the averaged experimental intensities of the outer satellites are greater and those of the inner satellites smaller than the calculated intensities. We assume, therefore, that the A spectrum is a combination of a Pb'_{Pb} pair signal and a Pb'_{Pb} single signal. In view of the fact that the inner satellites are only due to the resonance of the pair, the concentration ratio $[(Pb'_{Pb})_2]:[Pb'_{Pb}]$ can be estimated. One hour after the irradiation is stopped this ratio is 6:1. The intensity ratios of the lines calculated with the aid of this concentration ratio and the experimental intensity ratios agree very well.

Symmetry considerations in conjunction with the angular dependence measurements suggest that the Pb'_{Pb} pairs are oriented parallel to the [100] axis. Other types of pairs have various orientations in the crystal lattice. Their occurrence would result in a splitting of the A signal for most directions of H , which has not been observed.

Summarizing we can state that during irradiation single Pb'_{Pb} ions and pairs of Pb'_{Pb} ions are present in a distinct concentration ratio.

² We thank Dr. E. H. Hebeda of the Z.W.O. Laboratory for Isotope Geology in Amsterdam for carrying out the analysis.

After the irradiation is stopped the [Pb'_{Pb}], as well as the pair concentration, increases slowly with time up to a certain level.

5.3 The A Type Signal of PbBr₂

The A type signal is ascribed to anisotropic coupled Pb'_{Pb} pairs and single Pb'_{Pb} ions. In zero magnetic field the triplet levels of such an anisotropic coupled pair will split into a singlet and a doublet (18). If this splitting is much smaller than the microwave energy, the allowed transitions are just those within the triplet and two resonance lines will be observed. Consequently, three main lines will be measured if both single Pb'_{Pb} ions and pairs of Pb'_{Pb} ions are present. From a calculation of the position of the pair lines in the EPR spectrum it appears that they must be situated at equal distances from the single Pb'_{Pb} resonance line. This agrees with the experimental results (cf. Sect. 3.3). Due to hyperfine interaction each of the pair lines will be surrounded by four lines and the central line by two [the theoretical intensity ratios are the same as given in Eqs. (5.2.1) and (5.2.2)]. Unfortunately, the strength of the hyperfine lines is, with respect to the background of noise and other lines, too small to be able to check the intensity ratios of the lines. Additional evidence for this interpretation can be obtained from the fact that during an irradiation treatment, the strength of the A signal of both halides varied in a corresponding way. The different character of the pair coupling in PbCl₂ with respect to that in PbBr₂ and the absence of angular dependence of the A type signal of PbBr₂ are not well understood at the moment. Further optical and EPR investigations at low temperatures will be necessary to account for these phenomena.

5.4 The B Signal of PbCl₂ and PbBr₂

In accordance with Arends and Verwey (10), the B signal is ascribed to conduction electrons in colloidal lead particles. In PbCl₂ and sometimes in PbBr₂ we measured the typical asymmetric line shape of metallic particles with a diameter larger than the skin depth. The signal strength was almost constant in the temperature region 10–120°K (cf. Fig. 3 and Ref. (10)). This behavior is typical for a degenerate electron gas (10). The temperature dependence curve of the B signal of PbCl₂ shows an increase in the region 120–130°K, while this signal has disappeared at room temperature. This phenomenon is in

agreement with the optical absorption measurements on a PbCl₂ sample by Verwey (2). On warming up a sample irradiated at liquid nitrogen temperature an optical absorption band developed. This band, which has been ascribed to colloidal lead particles shifted to longer wavelength and bleached on further warming to room temperature (2).

5.5 The C Signal of PbCl₂

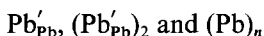
The positive shift ($\Delta g = +0.058$) of the *g* value of the C signal with respect to the free electron value indicates that the center concerned could carry a hole. Conductivity measurements on nominally pure PbCl₂ crystals (Bridgman technique) by De Vries (19, 20) in this laboratory showed that at room temperature the anion vacancy and cation vacancy concentrations are $\sim 10^{18}$ cm⁻³ and $< 10^{13}$ cm⁻³, respectively. The anion vacancy concentration is determined by extrinsic defects and, therefore, constant with decreasing temperature if no association occurs. The cation vacancy concentration decreases if the samples are cooled (20). Since the concentration of centers concerned in the C signal is 10²⁰ cm⁻³ (10°K) it is very improbable that holes trapped at cation vacancies or at associates of these vacancies with oppositely charged defects, could be the hole centers responsible for the C signal. In addition, the formation of new cation vacancies due to irradiation is improbable, since the occurrence of interstitial lead ions can be disregarded because of the relatively small radius of the interstitial spaces in PbCl₂ (20). In view of these considerations we assume that in the region 10–50°K (cf. Fig. 3), the holes are trapped at chloride ions. As chlorine has two stable isotopes, both with nuclear spin 3/2 and different nuclear moments, such a center is expected to give an EPR signal composed of several hyperfine lines. The structure observed on the C signal (see Sect. 3.2) could indicate that this signal is composed of a number of lines.

Finally it seems very improbable to us that the C signal originates from Pb'_{Pb}. The large hyperfine splitting due to the strong interaction between the 6*s* electron and the nucleus of the Pb'_{Pb} ion has not been observed in PbCl₂ (31, 32).

5.6 The Mechanism of the Photochemical Decomposition

Summarizing, we can state that the following defects are detected in PbCl₂ and PbBr₂ if single

crystals are irradiated with uv radiation at low temperatures:



In PbCl_2 , a hole center is created at liquid helium temperature. The Pb'_{Pb} center and the $(\text{Pb}'_{\text{Pb}})_2$ center are partly bleached by uv irradiation, whereas the $(\text{Pb})_n$ and the hole center of PbCl_2 are stable. All centers are destroyed during a warmup to room temperature. All phenomena can be reproduced in bleached samples.

Now we want to discuss the photochemical mechanism in both lead halides at low temperatures. Absorption of radiation of sufficiently short wavelength creates an electron hole pair



Since the holes are the dominant mobile charge carriers in PbCl_2 and PbBr_2 (23), we assume that a part of the photoelectrons will be trapped before recombination with the photoholes occurs.

Trapping Sites for Electrons

The number of anion vacancies is very small in comparison with the number of electrons that are trapped, viz.,

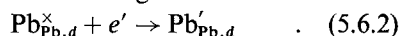
$$[V_{\text{Cl}}] \sim 10^{18} \text{ cm}^{-3} \text{ (20) and } [(\text{Pb}'_{\text{Pb}})_2]_{\text{PbCl}_2} \sim 4 \times 10^{20} \text{ cm}^{-3};$$

$$[V_{\text{Br}}] \sim 5 \times 10^{16} \text{ cm}^{-3} \text{ (21) and } [(\text{Pb}'_{\text{Pb}})_2]_{\text{PbBr}_2} \sim 5 \times 10^{18} \text{ cm}^{-3}.$$

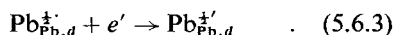
In addition, the formation of new anion vacancies due to irradiation is improbable using the same arguments as given *contra* the formation of new cation vacancies (see Sect. 5.5). The impurity concentration of the crystals is so low (17) that these defects also cannot be the sites where all the photoelectrons are trapped. We assume that dislocations play an important role as trapping sites for electrons. Dislocations are probably abundant under the surface due to cleaving (22, 27, 30).

Mitchell (24) suggested for AgBr that near the surface of the crystal halide ions at normal sites give rise to local occupied levels above the valence band, whereas Ag'_{Ag} ions give rise to empty levels below the conduction band, which corresponds to a narrowing of the forbidden gap at the surface. If the same would occur near internal surfaces (dislocations), this can possibly explain why dislocations can trap electrons as well as holes. If this model holds for PbCl_2 and

PbBr_2 , the trapping of the electrons occurs according to the following reaction:



In addition, it has been shown for AgBr that jogs in dislocations represent an effective positive charge of $\frac{1}{2}q$, i.e., the center can be designated by $\text{Ag}'_{\text{Ag},d}$ (11, 26). If the same occurs in PbCl_2 and PbBr_2 , trapping of the photoelectrons is represented by the reaction



The work of Layer et al. (35) on silver bromide showed that the visible latent image is not formed at nonjogged dislocations. A too low concentration of jogged dislocations may be an explanation for the fact that no defects could be measured on some of our PbCl_2 samples.

Defect Formation Due to Irradiation in the 3P_1 Cation Exciton Absorption Band

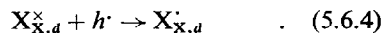
Irradiation into the 3P_1 cation exciton absorption band supplies the same photochemical results as does irradiation in the band edge (cf. Sect. 3.1). In the former case no free electrons and holes are created (23). The formation of defects due to irradiation into the 3P_1 cation exciton absorption band can be explained by the aforementioned suggestion of Mitchell. So, electron transfer will probably occur directly from halide ions to lead ions, both situated near dislocations.

Charge Compensation and Hole Trapping

It is known that in PbCl_2 and PbBr_2 the mass transport is carried by the anion vacancies (8). The mobility (μ) of the anion vacancies at 80 and 300°K has been calculated from the conductivity results of De Vries (19, 20) on PbCl_2 and of Schoonman (21) on PbBr_2 :

	$\mu_{V_{\text{Cl}}} \text{ (cm}^2 \text{ V}^{-1} \text{ s}^{-1})$	$\mu_{V_{\text{Br}}} \text{ (cm}^2 \text{ V}^{-1} \text{ s}^{-1})$
80°K	10^{-26}	10^{-16}
300°K	10^{-8}	10^{-6}

In view of these very low mobilities at 80°K and the relatively small concentrations of the anion vacancies (see above), it is very improbable that the charge compensation of the negative sites will occur by the anion vacancies. In PbCl_2 the concentration of hole centers detected at 10°K is $\sim 10^{20} \text{ cm}^{-3}$. The charge compensation probably occurs by trapping of holes at halide ions in the neighborhood of the trapped electrons. This is in agreement with the consideration mentioned above that halide ions near dislocations would be trapping sites for holes:



During the first irradiation period the concentration of Pb_{p_b}' and (Pb_{p_b}')₂ centers is small, as follows from the experimental results (cf. Sects. 3.2 and 3.3). These concentrations increase slowly with time after the irradiation is stopped, especially in PbCl₂. Now, we assume that the electrons trapped near dislocations [see Eq. (5.6.3)] do not give an EPR signal. Thereupon, the electrons and holes trapped near dislocations probably will migrate through the lattice until they are stabilized at normal lattice sites in Pb_{p_b}' single and pair centers near trapped hole centers. As a result the strength of the A signal increases. Repeated irradiation will cause a redistribution over the various traps and the conduction band leading to smaller Pb_{p_b}' and (Pb_{p_b}')₂ signals (cf. Fig. 2). In fact, the same situation as that at the end of the first irradiation period is reached. During subsequent "radiation off" and "radiation on" periods the processes described above will be repeated. The same holds for PbBr₂ crystals cleaved and mounted in the dark. We do not understand yet why in PbBr₂ this phenomenon can only be repeated a limited number of times (cf. Sect. 3.3).

An EPR signal due to hole centers has not been observed at 77°K. Since a pair of Pb_{p_b}' ions can be surrounded by two hole centers it may be that they are accommodated in a complex with paired electrons, e.g., (X_xX_x)^{••} or (X_xX_xX_x)^{••} (33, 34). Since the pair formation is strongly reduced in PbCl₂ at 10°K, it is likely that at this temperature mainly single hole centers giving the C signal are present. This model agrees with the results of the resonance measurements on PbBr₂, viz., irradiation at 10°K does not reduce the pair concentration significantly and no C type signal has been observed.

The calculations of the center concentrations are based on the assumption that the centers are only present in a surface layer of about 0.3 μm. This is the penetration depth of the electromagnetic radiation involved. This can be made plausible on the basis of the following:

- (1) Every time the irradiation is repeated the Pb_{p_b}' single and pair centers in PbCl₂ are bleached as a function of irradiation intensity (cf. Sect. 3.2);
- (2) The bleaching in the case of PbBr₂ can only be repeated for a limited number of times in crystals cleaved and mounted in the dark. However, the initially created concentration of centers does not increase due to prolonged irradiation (cf. Sect. 3.3).

We suppose that Pb_{p_b}' atoms are created at dislocations due to the disproportionation of the pairs according to



This reaction has already been suggested by Arends and Verwey (10). For the formation of metallic lead it is necessary to form colloids of lead atoms without enclosure of halide ions. This is possible at dislocations. The space required for this is obtained by slip along dislocations (25, 26). The space available at the dislocations for the colloids will be limited. So, a distinct number of colloid particles can be created and prolonged irradiation will not cause an increase of the number of lead particles (cf. Sect. 3.2).

The bleaching of the crystals during a warmup to room temperature can be explained by the following processes. First, the (Pb_{p_b}')₂ pairs form extra Pb_{p_b}' atoms at higher temperatures followed by an increase of the number of particles involved in the colloids (cf. Sect. 5.4). The space available for the colloids will probably increase with increasing temperature. Thereupon, holes will be thermally released from their traps and will recombine with lead particles and the remaining part of the Pb_{p_b}' and (Pb_{p_b}')₂ centers. We suppose that the recombination of holes with Pb_{p_b}' single and pair centers starts at lower temperatures if the warmup is carried out under irradiation of the samples (cf. Sect. 3.2 and Fig. 3).

Finally, we want to state that, in our opinion, the initial processes of the photolysis in PbCl₂ and PbBr₂ do not depend on temperature in the region investigated up to now, viz., 10–300°K (8). As the mobility of the anion vacancies is sufficiently large in the room temperature region a considerable number of new anion vacancies formed at the surface due to the desorption of halogen will diffuse into the crystal. This process agrees with the results of Verwey (see Sect. 1). So, the colloid formation in this region will be facilitated by the annihilation of these vacancies. At low temperatures, however, the desorption of halogen is strongly reduced because of the large decrease of the vacancy mobility. Consequently, the mechanism proposed by Verwey does not work anymore and the colloid formation can occur only at the dislocations.

6. Conclusions

The red luminescence of PbCl₂ and PbBr₂ at low temperatures is attributed to excitation and

radiative decay of Pb'_{Pb} or $(\text{Pb}'_{\text{Pb}})_2$ centers created by uv irradiation. On the basis of the results of this investigation it is difficult to determine whether the single center, the pair center, or both are responsible for the red luminescence. The excitation of the red luminescence probably occurs by one of the following mechanisms: excitation due to transport of exciting energy by resonance transfer or by diffusion and trapping of excitons (cf. Sect. 4). The yellow luminescence of PbCl_2 in the temperature region 10–40°K is ascribed to excitation and decay of Cl'_{Cl} centers.

Acknowledgments

The authors are very much indebted to Prof. Dr. G. Blasse and Prof. Dr. J. Volger for encouraging this work and for stimulating discussions and to Prof. Dr. J. H. van Santen for valuable criticism during the preparation of the manuscript. They gratefully acknowledge the assistance of Mr. G. H. van Driel with the EPR measurements.

References

1. W. C. DE GRUIJTER, *Phys. Lett. A* **34**, 251 (1971).
2. J. F. VERWEY, Thesis, Utrecht, **71**, 73 (1971).
3. W. C. TENNANT, *J. Phys. Chem.* **70**, 3523 (1966).
4. H. L. WELLS, *Amer. J. Sci.* **45**, 134 (1893).
5. R. S. NORRIS, *Amer. Chem. J.* **17**, 191 (1895).
6. A. K. SANYAL AND N. R. DHAR, *Z. Anorg. Chem.* **128**, 212 (1923).
7. C. RENZ, *Z. Anorg. Chem.* **116**, 62 (1921).
8. J. F. VERWEY, *J. Phys. Chem. Solids* **31**, 163 (1970).
9. J. D. KONITZER AND H. N. HERSH, *J. Phys. Chem. Solids* **27**, 771 (1966).
10. J. ARENDS AND J. F. VERWEY, *Phys. Status Solidi* **23**, 137 (1967).
11. F. A. KRÖGER, "The Chemistry of Imperfect Crystals," North-Holland Publ. Co., Amsterdam (1964).
12. D. POOLEY, *Proc. Phys. Soc. London* **87**, 245 (1966).
- 13a. J. F. VERWEY AND J. SCHOONMAN, *Physica (Utrecht)* **35**, 386 (1967).
- 13b. B. WILLEMSEN, *J. Solid State Chem.* **3**, 567 (1971).
14. J. KERSSSEN, (unpublished).
15. R. H. WEBB, *Phys. Rev.* **158**, 225 (1967).
16. W. C. DE GRUIJTER, "International Conference on Colour Centres in Ionic Crystals," Reading, U.K., 204 (1971).
17. W. C. DE GRUIJTER, *J. Solid State Chem.*, accepted for publication.
18. A. ABRAGAM AND B. BLEANY, "Electron Paramagnetic Resonance of Transition Ions," p. 502, Clarendon Press, Oxford (1970).
19. K. J. DE VRIES AND J. H. VAN SANTEN, *Physica (Utrecht)* **29**, 482 (1963); **30**, 2051 (1964).
20. K. J. DE VRIES, Thesis, University of Utrecht (1965).
21. J. SCHOONMAN, *J. Solid State Chem.* **4**, 466 (1972).
22. J. J. GILMAN AND W. G. JOHNSTON, *Solid State Phys.* **13**, 147 (1962).
23. J. F. VERWEY AND N. G. WESTERINK, *Physica (Utrecht)* **42**, 293 (1969).
24. J. W. MITCHELL, *Rep. Prog. Phys.* **20**, 468 (1958).
25. A. S. PARASNIS AND J. W. MITCHELL, *J. Photogr. Sci.* **4**, 171 (1959).
26. F. SEITZ, *Rev. Mod. Physics* **23**, 328 (1951); "Imperfections in nearly perfect crystals," p. 3, John Wiley and Sons, New York (1952).
27. J. T. BARTLETT AND J. W. MITCHELL, *Phil. Mag.* **5**, 445 (1960).
28. K. J. BEST, *Z. Phys.* **163**, 309 (1961).
29. E. ILMAS, R. KINK, G. LIIDJA, AND A. MALYSHEVA, *Tr. Inst. Fiz. Astron. Akad. Nauk. Est. S.S.R.* **26**, 112 (1963).
30. C. B. CHILDS, *Phys. Rev. Lett.* **5**, 502 (1960).
31. D. SCHOEMAKER AND J. L. KOLOPUS, *Solid State Commun.* **8**, 435 (1970).
32. G. BORN, A. HOFSTAETTER, AND A. SCHARMANN, *Z. Phys.* **245**, 333 (1971).
33. J. SCHNEIDER, B. DISCHLER, AND A. RÄUBER, *Phys. Status Solidi* **13**, 141 (1966).
34. S. SCHLICK, *Chem. Phys. Lett.* **4**, 421 (1969).
35. H. LAYER, M. G. MILLER, AND L. SLIFKIN, *J. Appl. Phys.* **33**, 478 (1962); H. LAYER AND L. SLIFKIN, *J. Phys. Chem.* **66**, 2396 (1962).
36. W. C. DE GRUIJTER AND J. KERSSSEN, *Solid State Commun.* **10**, 837 (1972).